

# Mitochondrial Single-stranded DNA-binding Proteins Stimulate the Activity of DNA Polymerase $\gamma$ by Organization of the Template DNA\*

Received for publication, June 20, 2015, and in revised form, October 5, 2015. Published, JBC Papers in Press, October 7, 2015, DOI 10.1074/jbc.M115.673707

Grzegorz L. Ciesielski<sup>‡§1,2</sup>, Oya Bermek<sup>¶1</sup>, Fernando A. Rosado-Ruiz<sup>§</sup>, Stacy L. Hovde<sup>§</sup>, Orrin J. Neitzke<sup>§</sup>, Jack D. Griffith<sup>¶</sup>, and Laurie S. Kaguni<sup>‡§3</sup>

From the <sup>‡</sup>Institute of Biosciences and Medical Technology, University of Tampere, 33520 Tampere, Finland, the <sup>§</sup>Department of Biochemistry and Molecular Biology and Center for Mitochondrial Science and Medicine, Michigan State University, East Lansing, Michigan 48823, and the <sup>¶</sup>Lineberger Comprehensive Cancer Center, University of North Carolina, Chapel Hill, North Carolina 27514

**Background:** mtSSB stimulates the activity of Pol  $\gamma$ .

**Results:** Stimulation of Pol  $\gamma$  activity by SSB correlates with the organization of ssDNA templates in a species-independent manner.

**Conclusion:** Organization of the template DNA by mtSSB is the major factor contributing to the stimulation of Pol  $\gamma$  activity.

**Significance:** This study provides insight into the functional relationship of Pol  $\gamma$  and mtSSB and a general mechanism for it.

The activity of the mitochondrial replicase, DNA polymerase  $\gamma$  (Pol  $\gamma$ ) is stimulated by another key component of the mitochondrial replisome, the mitochondrial single-stranded DNA-binding protein (mtSSB). We have performed a comparative analysis of the human and *Drosophila* Pols  $\gamma$  with their cognate mtSSBs, evaluating their functional relationships using a combined approach of biochemical assays and electron microscopy. We found that increasing concentrations of both mtSSBs led to the elimination of template secondary structure and gradual opening of the template DNA, through a series of visually similar template species. The stimulatory effect of mtSSB on Pol  $\gamma$  on these ssDNA templates is not species-specific. We observed that human mtSSB can be substituted by its *Drosophila* homologue, and *vice versa*, finding that a lower concentration of insect mtSSB promotes efficient stimulation of either Pol. Notably, distinct phases of the stimulation by both mtSSBs are distinguishable, and they are characterized by a similar organization of the template DNA for both Pols  $\gamma$ . We conclude that organization of the template DNA is the major factor contributing to the stimulation of Pol  $\gamma$  activity. Additionally, we observed that human Pol  $\gamma$  preferentially utilizes compacted templates, whereas the insect enzyme achieves its maximal activity on open templates, emphasizing the relative importance of template DNA organization in modulating Pol  $\gamma$  activity and the variation among systems.

The presence of mtSSB<sup>4</sup> is a hallmark of replicating mitochondrial nucleoids (1). Together with mitochondrial DNA

helicase (also known as Twinkle) and the mitochondrial replicase, Pol  $\gamma$ , it reconstitutes a minimal replisome for human mitochondria (2). Knockdown of mtSSB in human HeLa cells results in reduction of mitochondrial DNA (mtDNA) copy number due to a decrease in mtDNA synthesis (3), as was reported earlier for *Drosophila* Schneider cells in culture (4). Moreover, *lopo* mutants of *Drosophila melanogaster* in which mtSSB is absent die at an early stage in development, concomitant with the complete loss of mtDNA and respiratory capacity (5).

The presence of mtSSB at the displacement loop structure of mtDNA inhibits its resolution *in vitro* by the transcriptional activator and mtDNA compaction protein TFAM (6). Moreover, mtDNA helicase and Pol  $\gamma$  bind and utilize efficiently mtSSB-coated single-stranded DNA (ssDNA) (7, 8). The *Escherichia coli* homologue of mtSSB (*EcSSB*) has been demonstrated to act as a platform to recruit its interacting partners in bacterial DNA replication (9, 10), which implies that mtSSB may also serve this function in the mtDNA replication process.

The importance of SSBs in DNA replication extends beyond the initiation phase. SSB proteins enhance helix destabilization by DNA helicases, prevent reannealing of the separated ssDNA strands, and protect them from nuclease digestion (11). Numerous DNA polymerases have been shown to function in concert with SSB, thereby increasing their rates of nucleotide incorporation and processivity. Such a functional relationship has also been demonstrated for mitochondrial SSB and Pol  $\gamma$  proteins (12–14). Possible mechanisms for the stimulatory effects of SSBs have emerged, suggesting either a direct physical interaction with their partner Pols or their passive interaction with template DNA (11, 15).

Pol  $\gamma$  dysfunction is the major cause of human mitochondrial diseases, for which there is no direct treatment currently available (16). Understanding how mtSSB stimulates Pol  $\gamma$  may contribute to developing treatment strategies based on enhancing

\* This work was supported by National Institutes of Health Grants GM45295 (to L. S. K.) and GM31819 and ES13773 (to J. D. G.). The authors declare that they have no conflicts of interest with the contents of this article.

<sup>1</sup> These authors contributed equally to this work.

<sup>2</sup> Supported by the University of Tampere.

<sup>3</sup> To whom correspondence may be addressed: Dept. of Biochemistry and Molecular Biology and Center for Mitochondrial Science and Medicine, Michigan State University, 603 Wilson Rd., East Lansing, MI 48823. Tel.: 517-353-6703; Fax: 517-353-9334; E-mail: lskaguni@msu.edu.

<sup>4</sup> The abbreviations used are: mtSSB, mitochondrial SSB; SSB, single-stranded DNA-binding protein; Pol, DNA polymerase; mtDNA, mitochondrial DNA; DmmtSSB, *D. melanogaster* mtSSB; HsmtSSB, human mtSSB; EcSSB, *E. coli*

SSB; DmPol  $\gamma$ , *D. melanogaster* Pol  $\gamma$ ; HsPol  $\gamma$ , human Pol  $\gamma$ ; nt, nucleotide(s); l2,3, loop 2,3; Hsl2,3, human l2,3; Dm12,3, *D. melanogaster* l2,3.

## Mechanism of Stimulation of Pol $\gamma$ Activity by mtSSB

Pol  $\gamma$  activity. We sought to assess the mechanism of the stimulatory effect of human mtSSB on its cognate Pol  $\gamma$ . We recently published a comparative analysis of Pol  $\gamma$  sequences and structural organization from various metazoan taxa (17) and included in this study homologous proteins from *D. melanogaster* and *E. coli* to examine similarities and differences between these systems. Our current findings provide evidence of a relationship between Pol  $\gamma$  activity and SSB-generated template DNA organization.

### Experimental Procedures

**Nucleotides and Nucleic Acids**—Unlabeled deoxyribonucleotides were purchased from Qiagen. [ $\alpha$ - $^{32}$ P]dCTP was purchased from PerkinElmer Life Sciences. Bacteriophage M13 DNA (6,407 nt) used for biochemical studies was prepared by standard laboratory methods, and M13mp18 DNA used for electron microscopic analyses was purchased from New England Biolabs. A 15-mer oligodeoxynucleotide complementary to M13 DNA was synthesized in an Applied Biosystems oligonucleotide synthesizer and then used to prepare the singly primed M13 DNA for DNA polymerase assays as described previously (18). The 48-mer oligodeoxynucleotide used in gel mobility shift assays was as described previously (19).

**Proteins**—Recombinant human and *D. melanogaster* mtSSB proteins were prepared from bacterial cells as described previously (20), except that the glycerol gradient centrifugation step was replaced by gel filtration as follows. Fraction IIb was chromatographed on a Superdex 75 gel filtration column equilibrated with buffer containing 50 mM Tris-HCl, pH 7.5, 8% glycerol, 150 mM KCl, 2 mM EDTA at a flow rate of 1 ml/min at 4 °C. Fractions containing the mtSSBs were pooled (fraction III) and dialyzed against buffer containing 35 mM Tris-HCl, pH 7.5, 8% glycerol, 100 mM NaCl, 2 mM EDTA, 2 mM dithiothreitol. Recombinant catalytic subunit of human Pol  $\gamma$  (Pol  $\gamma\alpha$ ) and *Drosophila* Pol  $\gamma$  holoenzyme were prepared from Sf9 cells as described previously (20). Recombinant accessory subunit of human Pol  $\gamma$  (Pol  $\gamma\beta$ ) was prepared from bacterial cells as described previously (20). Recombinant *E. coli* SSB protein was purchased from Affymetrix.

**Mutagenesis of DmmtSSB**—Mutagenesis was performed in the pMt/Hy vector to generate the *Drosophila* mtSSB loop 2,3 variant as described previously (7). The open reading frame was amplified by PCR with the forward 5'-ATACATATGGCAAC-AACAACAACGGCAGCGGCT-3' and reverse 5'-TATAGATCTTTAGTTGTTGGCATCACGAAAAACAA-3' primers. The insert was digested with NdeI and BglII and ligated into the pET-11a vector digested with NdeI and BamHI. DNA sequence analysis was performed to confirm the structure and sequence integrity of the resulting plasmid.

**DNA Polymerase  $\gamma$  Stimulation Assay**—Reaction mixtures of 50  $\mu$ l (Fig. 1) or 25  $\mu$ l (Figs. 3, 4, and 6) total volume contained 50 mM Tris-HCl, pH 8.5, 4 mM MgCl<sub>2</sub>, 400  $\mu$ g/ml bovine serum albumin, 10 mM dithiothreitol, 30 mM KCl, 20  $\mu$ M each dGTP, dATP, dCTP, and dTTP, [ $\alpha$ - $^{32}$ P]dCTP (2  $\mu$ Ci), and the amounts of singly primed M13 DNA and proteins that are indicated in the legends for Figs. 1, 3, 4 and 6. Incubation was at 37 °C for 30 min. Samples were processed, and nucleotide incorporation was quantified in a liquid scintillation counter.

**Analysis of Products of DNA Synthesis by Gel Electrophoresis**—Reaction mixtures of 50- $\mu$ l total volume contained 50 mM Tris-HCl, pH 8.5, 4 mM MgCl<sub>2</sub>, 400  $\mu$ g/ml bovine serum albumin, 10 mM dithiothreitol, 30 mM KCl, 20  $\mu$ M each dGTP, dATP, and dTTP, 5  $\mu$ M dCTP, [ $\alpha$ - $^{32}$ P]dCTP (20  $\mu$ Ci), and the amounts of singly primed M13 DNA and proteins that are indicated in the legend for Fig. 1. Incubation was at 30 °C for 30 min. The reaction products were isolated and analyzed by gel electrophoresis and autoradiography, as described by Williams and Kaguni (18), except that equal aliquots of the total DNA isolated were loaded on the gel.

**ssDNA Binding and Gel Mobility Shift Assay**—Reaction mixtures (20  $\mu$ l) contained 20 mM Tris-HCl, pH 7.5, 1 mM dithiothreitol, 4 mM MgCl<sub>2</sub>, 50 mM NaCl, 36 fmol of 5'- $^{32}$ P-end labeled 48-mer, and the indicated amounts of the DmmtSSB proteins. Incubation was at 20 °C for 10 min. Samples were processed, electrophoresed in 6% native polyacrylamide gels, and analyzed by autoradiography. The amounts of shifted and free oligonucleotide were quantitated as follows: percentage of ssDNA bound =  $(V_S / (V_S + V_F)) \times 100$ , where  $V_S$  represents the volume of the shifted and  $V_F$  is the volume of unshifted oligonucleotide in the sample lane of interest.

**Electron Microscopy**—Samples (50  $\mu$ l) of mtSSB bound to M13mp18 DNA were prepared by incubating the DNA (1  $\mu$ g/ml) with various amounts of mtSSB in 10 mM HEPES, pH 7.6, 4 mM MgCl<sub>2</sub>, and 50 mM NaCl for 20 min at room temperature. Glutaraldehyde was added to 0.6% for 5 min at room temperature to fix the structures, and the samples were chromatographed over 2-ml columns of 6% agarose beads (Agarose Bead Technologies) equilibrated in 10 mM Tris-HCl (pH 7.6) and 0.1 mM EDTA. The samples were then adsorbed to thin carbon supports in the presence of 2 mM spermidine, washed, air-dried, and rotary shadow-cast with tungsten as described (21). Samples were examined using an FEI Tecnai T12 electron microscope at 40 kV. Length measurements were made by capturing the electron microscopic images with a Gatan Orius CCD camera and using Gatan Digital Micrograph software. Contrast in the images was adjusted in Adobe Photoshop and arranged into panels (21).

### Results

**DNA Polymerization Activity of Pol  $\gamma$  Depends on the Molar Relationship of mtSSB and Template DNA**—To evaluate the mechanism of stimulation of HsPol  $\gamma$  activity by HsmtSSB, we first examined the effect of SSB concentration under standard assay conditions in template DNA excess. We found that the extent of stimulation of DNA synthesis by Pol  $\gamma$  fluctuates characteristically with increase in the mtSSB concentration (Fig. 1 left, open circles). Low concentrations of mtSSB have no effect ("limiting mtSSB"), but over a threshold level, mtSSB begins to stimulate the activity of Pol  $\gamma$  ("initial stimulation") to achieve its maximal efficiency ("maximal stimulation"). Upon further increase in the mtSSB concentration, the stimulatory effect is reduced markedly ("inhibition"). When we reduced the template DNA concentration by 10-fold, we observed that the individual phases of stimulation occur at similar ratios of SSB molecules to the template DNA (closed circles). This observation

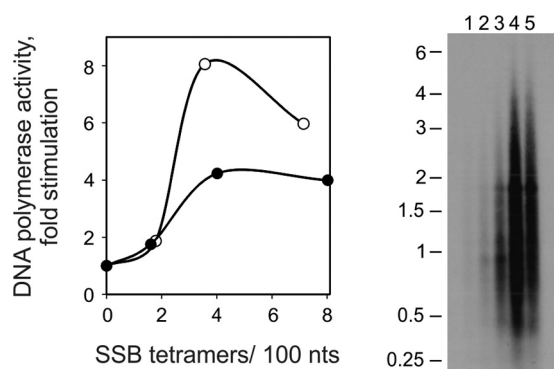


**FIGURE 1. Stimulation of DNA polymerase activity of HsPol  $\gamma$  upon increasing molar ratio of HsmtSSB to template M13 DNA.** *Left*, DNA polymerase stimulation assay. The DNA polymerase assay was performed as described under “Experimental Procedures,” using 23 fmol (closed circles) or 230 fmol (open circles) of singly primed M13 DNA, 70 fmol of HsPol  $\gamma\alpha$ , 430 fmol of HsPol  $\gamma\beta$ , and increasing amounts of HsmtSSB: 0, 3, 6, and 12 pmol for 23 fmol of template or 0, 27, 53, and 107 pmol for 230 fmol of template. Assays were performed at 30 mM KCl and 4 mM MgCl<sub>2</sub>. The data were normalized to the amount of nucleotide incorporated by HsPol  $\gamma$  in the absence of SSB (arbitrarily set to 1 in each case). *Right*, gel analysis of products of DNA synthesis. DNA synthesis was performed as described under “Experimental Procedures,” using 117 fmol of singly primed M13 DNA; 71.5 fmol of Pol  $\gamma\alpha$ ; 436 fmol of Pol  $\gamma\beta$ ; and 0, 13, 21, 32, and 64 pmol of wild-type HsmtSSB (lanes 1–5, respectively). DNA product strands were isolated, denatured, and electrophoresed in a denaturing 1.5% agarose gel, which was autoradiographed.

implies that Pol  $\gamma$  stimulation is dictated by the SSB/template DNA ratio.

We also examined the products of DNA synthesized by HsPol  $\gamma$  at the molar ratios of HsmtSSB to the template DNA corresponding to those we used for the stimulation assay (Fig. 1, right). In parallel with the stimulation profiles, we observed that mtSSB predominantly enhances primer utilization to increase the extent of DNA synthesis, with only a modest effect on DNA product strand length, which we determined in this analysis to be  $\sim$ 760 nt in the absence of mtSSB up to  $\sim$ 1100 nt in its presence. This effect is similar to that described previously for Pol  $\gamma$  from *D. melanogaster* and with the processivity of human Pol  $\gamma$  calculated from single nucleotide incorporation assays (12, 22, 23).

**mtSSB Organizes the ssDNA Template**—We employed electron microscopy (EM) to examine how an increase in HsmtSSB concentration affects the template DNA structure. We found that HsmtSSB organizes the ssDNA template; an increase in HsmtSSB concentration leads to a dissolution of secondary structures and gradual opening of the template DNA (Fig. 2). We distinguished several characteristic species. At concentrations of HsmtSSB below saturation of the template DNA, as predicted from the ssDNA binding site size for vertebrate mtSSB tetramers of 35 nt (13, 24, 25), the template maintains a compacted structure. Binding of SSB results in the appearance of the forms called “beaded” and “collapsed.” When the concentration of mtSSB exceeds that required to saturate all of the template DNA molecules, we observed a transition from collapsed to open species, through a series of partially opened intermediates. The open stretch in the template DNA structure of the intermediates enlarges with further increase in the HsmtSSB concentration. Interestingly, the template reaches a fully open form at an HsmtSSB concentration  $\sim$ 3-fold higher (by calculation) than that required (by calculation) to saturate

all of the template DNA molecules. The contour length of the open species is 0.099 nm/nt on average, which is over 3-fold less than that of the double-stranded (replicative) form of the M13 phage genome (0.34 nm/nt).

**The Activity of Pol  $\gamma$  Depends on Template DNA Organization**—In our earlier studies, we identified several structures observed in the crystal structure (26) of HsmtSSB that are important for the stimulation of HsPol  $\gamma$  activity (7). In the case of *D. melanogaster* mtSSB (DmmtSSB), these structures are either missing (e.g. the loop 2,3 structure is reduced from nine to three amino acids), or the sequence is altered significantly (e.g. the  $\alpha$ 1 helix). Nonetheless, DmmtSSB is able to stimulate efficiently the activity of its partner Pol  $\gamma$  (DmPol  $\gamma$ ) (27). We cross-tested the ability of DmmtSSB and HsmtSSB to stimulate their orthologous Pols and found that, despite their structural differences, DmmtSSB is able to stimulate HsPol  $\gamma$  as efficiently as HsmtSSB (Fig. 3A). In addition, HsmtSSB is able to stimulate DmPol  $\gamma$  as efficiently as DmmtSSB (Fig. 3B). We found that the degree of DmPol  $\gamma$  stimulation is  $\sim$ 10-fold greater than that of HsPol  $\gamma$  (Fig. 3, compare A and B). This difference results from a significantly lower initial activity of DmPol  $\gamma$  in comparison with HsPol  $\gamma$ . However, at the peaks of stimulation, both Pols produce a comparable amount of nascent DNA (Fig. 3C). HsPol  $\gamma$  reaches its maximal stimulation at a ratio of  $\sim$ 4.5 HsmtSSB tetramers/100 nt, whereas  $\sim$ 3 DmmtSSB tetramers per 100 nt are sufficient (Fig. 3, A and B). Also, the inhibition phase occurs at lower concentration and is more dramatic in the case of DmmtSSB (Fig. 3A). Notably, whereas DmPol  $\gamma$  reaches its maximal stimulation at a ratio of  $\sim$ 4.5 DmmtSSB tetramers/100 nt, 9 HsmtSSB tetramers are required per 100 nt (Fig. 3B), and HsmtSSB does not inhibit the activity of DmPol  $\gamma$  within the concentration range utilized. We believe this is a result of the lower efficiency of template organization by HsmtSSB. Given that the stimulation profiles for both Pols with their cognate SSBs are highly similar (e.g. the maximal stimulation of HsPol  $\gamma$  by HsmtSSB and that of DmPol  $\gamma$  by DmmtSSB both occur at  $\sim$ 4.5 mtSSB tetramers per 100 nt (Fig. 3, compare A and B)), this implies that there are significant differences between the properties of the DmmtSSB and HsmtSSB that are required to achieve a stimulatory effect on Pol  $\gamma$ .

To evaluate the putative relationship between the ability of mtSSB to organize the template DNA and to stimulate Pol  $\gamma$  activity, we examined by electron microscopy the template species formed at HsmtSSB/template ratios representing specific phases of the HsPol  $\gamma$  stimulatory profile (Fig. 3, A and D, and Table 1). In the limiting mtSSB phase that occurs below saturation of the template DNA molecules,  $\sim$ 70% of the molecules do not appear to be significantly different from the template alone. In the initial stimulation phase, we observed formation of the collapsed molecules, which were predominant among others. At the peak of stimulation of HsPol  $\gamma$ , we observed a mixture of the collapsed (38%) and the partially open forms (55%). At a ratio representing the inhibitory phase, we observed a mixture of partially (41%) and fully open molecules (54%). Next, we tested how the substitution of HsmtSSB with its *D. melanogaster* orthologue affects the template organization (Fig. 3D). We found that increasing DmmtSSB concentration results in

## Mechanism of Stimulation of Pol $\gamma$ Activity by mtSSB

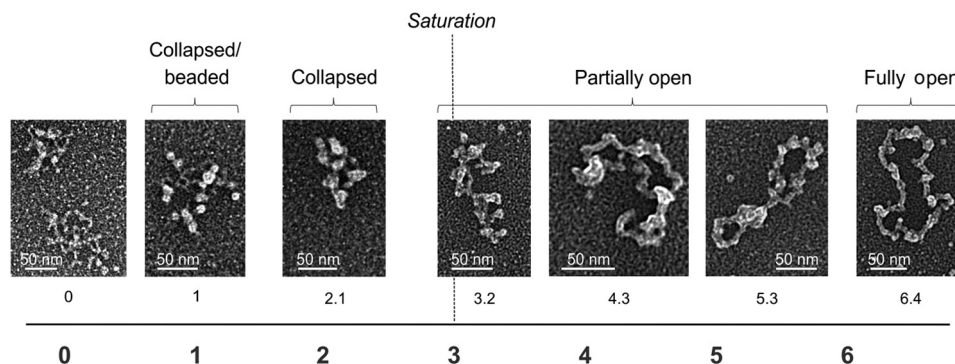


FIGURE 2. **Electron microscopy of human wild-type mtSSB protein bound to the M13 DNA template.** The binding reaction was performed at 30 mM KCl and 4 mM MgCl<sub>2</sub>. The numbers below individual images indicate the ratio of SSB tetramers per 100 nucleotides of template DNA. The dashed line indicates the concentration of SSB tetramers that would result in saturation of the template DNA molecules (as predicted from the ssDNA binding site size of 35 nt/tetramer). The following species were distinguished: collapsed/beaded, collapsed, partially open, and fully open.

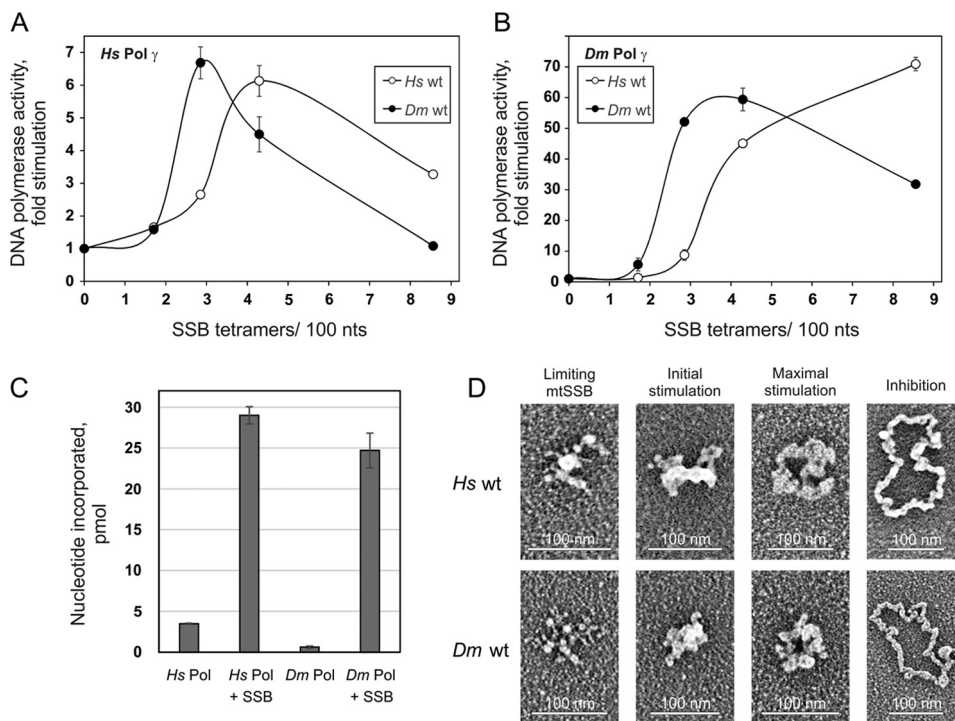


FIGURE 3. **Individual phases of Pol  $\gamma$  stimulation correlate with a specific template organization.** A and B, a DNA polymerase assay was performed as described under "Experimental Procedures," using 58.5 fmol of singly primed M13 DNA; 35 fmol of *HsPol*  $\gamma\alpha$ ; 220 fmol of *HsPol*  $\gamma\beta$  (A) or 40 fmol of *DmPol*  $\gamma$  (as *Pol*  $\gamma\alpha$ ) (B); and 0, 6.4, 10.7, 16, or 32 pmol of either *H. sapiens* (open circles) or *D. melanogaster* (closed circles) wild-type mtSSB. Assays were performed at 30 mM KCl and 4 mM MgCl<sub>2</sub>. The data were normalized to the amount of nucleotide incorporated by *HsPol*  $\gamma$  in the absence of mtSSB (arbitrarily set to 1 in each case). C, comparison of nucleotide incorporation by *H. sapiens* or *D. melanogaster* Pol  $\gamma$  in the absence or presence of the wild-type *D. melanogaster* mtSSB at the concentrations resulting in maximal stimulation: 10.7 pmol for *HsPol*  $\gamma$  and 16 pmol for *DmPol*  $\gamma$ . D, electron microscopy of *H. sapiens* (top) and *D. melanogaster* (bottom) wild-type mtSSB proteins on M13 DNA. The binding reaction was performed at 30 mM KCl and 4 mM MgCl<sub>2</sub>. The images are representative of template species formed at the following ratios of SSB tetramers per 100 nucleotides, which correspond to the indicated individual phases of the stimulation of *HsPol*  $\gamma$  activity: limiting mtSSB, 1.6 *HsmtSSB* and 1.2 *DmmtSSB*; initial stimulation, 3.2 *HsmtSSB* and 1.8 *DmmtSSB*; maximal stimulation, 3.8 *HsmtSSB* and 2.5 *DmmtSSB*; inhibition, 6.4 *HsmtSSB* and 7 *DmmtSSB* (also see Table 1). Error bars, S.D.

the appearance of template DNA species similar to those observed for *HsmtSSB*. In the presence of limiting *DmmtSSB*, a fraction of template DNA transits from forms that are indistinguishable from the unbound template to the collapsed/beaded species. A further increase in the *DmmtSSB* concentration to a level greater than required for saturation of the template DNA molecules results in gradual opening of the template. In contrast to *HsmtSSB*, the transition between the forms of template species is systematically shifted toward lower concentrations of *DmmtSSB*. This shift correlates with a shift in the peak of *HsPol*  $\gamma$  stimulation toward lower concentrations of *DmmtSSB*. From

this correlation we conclude that despite the differences between their stimulatory profiles, each phase of the *DmmtSSB* profile corresponds to a composition of template DNA species similar to those for *HsmtSSB*. The majority of template DNA molecules in the limiting mtSSB phase (63%) are not significantly different from the template alone. In the initial stimulation phase, the template DNA is predominantly converted into collapsed forms. At the peak of *HsPol*  $\gamma$  stimulation, we observed a mixture of the collapsed and the partially open forms of the template DNA, contributing 35 and 53%, respectively. The inhibition phases of the *HsPol*  $\gamma$  stimulation profile

TABLE 1

Distribution of template species formed by SSB/template DNA ratios corresponding to specific phases of the *HsPol*  $\gamma$  stimulation profile

The percentage distribution of template forms generated by SSB variants was determined by transmission electron microscopy. Samples representative of the various phases of the stimulation profiles were prepared as described under "Experimental Procedures." The underlining indicates the predominant template DNA species at a given phase of the stimulation profile.

Stimulation phase (SSB tetramers/100 nt)	No difference	Collapsed/beaded	Collapsed	Partially open	Fully open
<b><i>HsmtSSB</i></b>					
Limiting mtSSB (1)	<u>77</u>	17	3	4	0
Limiting mtSSB (1.6)	<u>68</u>	18	9	5	0
Initial stimulation (3.2)	6	9	<u>60</u>	25	0
Maximal stimulation (3.8)	0	0	38	<u>55</u>	7
Inhibition (6.4)	0	0	5	41	<u>54</u>
<b><i>DmmtSSB</i></b>					
Limiting mtSSB (1.2)	<u>63</u>	36	1	0	0
Initial stimulation (1.8)	0	0	<u>62</u>	38	0
Maximal stimulation (2.5)	0	0	35	<u>53</u>	12
Inhibition (3.5)	0	0	0	16	<u>84</u>
Inhibition (7)	0	0	0	0	<u>100</u>
<b><i>HsmtSSB</i> loop 2,3</b>					
Limiting mtSSB (1.1)	90	3	5	2	0
Limiting mtSSB (1.7)	<u>73</u>	11	14	2	0
Initial stimulation (3.4)	8	<u>45</u>	39	8	0
Maximal stimulation (4)	0	0	35	<u>53</u>	12
Inhibition (6.8)	0	0	19	<u>70</u>	11
<b><i>DmmtSSB</i> loop 2,3</b>					
Limiting mtSSB (1.2)	<u>76</u>	20	2	2	0
Initial stimulation (1.8)	<u>26</u>	24	<u>28</u>	22	0
Maximal stimulation (2.5)	0	0	16	<u>60</u>	24
Inhibition (3.6)	0	0	2	27	<u>71</u>
Inhibition (7.2)	0	0	0	0	<u>100</u>
<b><i>EcSSB</i></b>					
Initial stimulation (0.85)	0	<u>62</u>	34	3	1
Initial stimulation (1.3)	0	21	<u>61</u>	18	0
Maximal stimulation (2.6)	0	0	1	33	<u>66</u>
Plateau (5.1)	0	0	0	0	<u>100</u>
Plateau (7.7)	0	0	0	0	<u>100</u>

by the *HsmtSSB* and the *DmmtSSB* differ such that *HsmtSSB* is less inhibitory than *DmmtSSB*. This difference appears to correlate with a relatively higher composition of the fully open forms of the template DNA at the various SSB/template ratios for *DmmtSSB*. For *DmmtSSB*, a ratio of 3.5 SSB tetramers/100 nt renders 84% of template molecules fully open, and this value increases up to 100% at a ratio of 7 SSB tetramers/100 nt. By comparison, an *HsmtSSB* ratio of 6.4 SSB tetramers/100 nt yields an approximately equal mixture of partially and fully open forms. On the other hand, in evaluating the *DmPol*  $\gamma$  stimulation profiles, we noticed that an increase in the fraction of the fully open template DNA molecules generated by *HsmtSSB* corresponds with an increase of *DmPol*  $\gamma$  activity, whereas an increase of the same species generated by *DmmtSSB* corresponds with a decrease in *DmPol*  $\gamma$  activity (Fig. 3, compare *B* with *D*, and corresponding values in Table 1). Taken together with the differences in the template DNA opening efficiency, this might indicate that the DNA complexes generated by *DmmtSSB* or *HsmtSSB* have different molecular properties, which could relate simply to the overall differences in their amino acid sequences.

**The Activity of Pol  $\gamma$  Does Not Depend Directly on the Loop 2,3 Structure of *HsmtSSB***—We have shown previously that the *HsmtSSB* loop 2,3 variant (*Hsl2,3*), which bears a deletion of the loop 2,3 structure, is unable to stimulate *HsPol*  $\gamma$  activity (7) (Fig. 4A). Because native *DmmtSSB* has a limited loop 2,3 structure, we tested whether *Hsl2,3* is able to stimulate *DmPol*  $\gamma$ . We found that at a ratio of  $\sim$ 3–5 SSB tetramers/100 nt, which cor-

responds to the initial phase of stimulation of *DmPol*  $\gamma$  by wild-type *HsmtSSB*, the *Hsl2,3* variant is also able to stimulate *DmPol*  $\gamma$  to some extent (compare Fig. 4B with Fig. 3B). However, in contrast to the wild-type protein, a further increase in the *Hsl2,3* concentration does not result in increased stimulation of *DmPol*  $\gamma$  activity, and as a result, the enzyme does not reach the maximal stimulation phase (compare Fig. 4B with Fig. 3B at 9 SSB tetramers/100 nt). Next, we asked whether the inability of the *HsmtSSB* 12,3 variant to stimulate efficiently both Pols is also related to the template DNA organization (Fig. 4C and Table 1). At ratios of SSB tetramers per 100 nt that correspond to the limiting mtSSB phase of the stimulation profile for the wild-type protein, we observed that the vast majority of template DNA molecules are not significantly different from the template DNA in the absence of mtSSB. At ratios corresponding to the initial stimulation phase for the wild-type protein, we observed a mixture of the partly collapsed (collapsed/beaded) and collapsed forms. At a ratio corresponding to the peak in the wild-type mtSSB stimulation profile, we observed that the *Hsl2,3* variant forms a mixture of collapsed and partially open molecules at levels of 35 and 53%, respectively. Further increase in the *Hsl2,3* variant concentration results in an increase of the partially open forms (up to 70%). We observed that over the range of concentrations examined, the *HsmtSSB* 12,3 variant is unable to open efficiently the template DNA molecules because the fraction of the fully open molecules does not exceed 12% (as compared with 54% for the wild-type protein). Notably, the fully open molecules are nearly 5-fold shorter than

## Mechanism of Stimulation of Pol $\gamma$ Activity by mtSSB

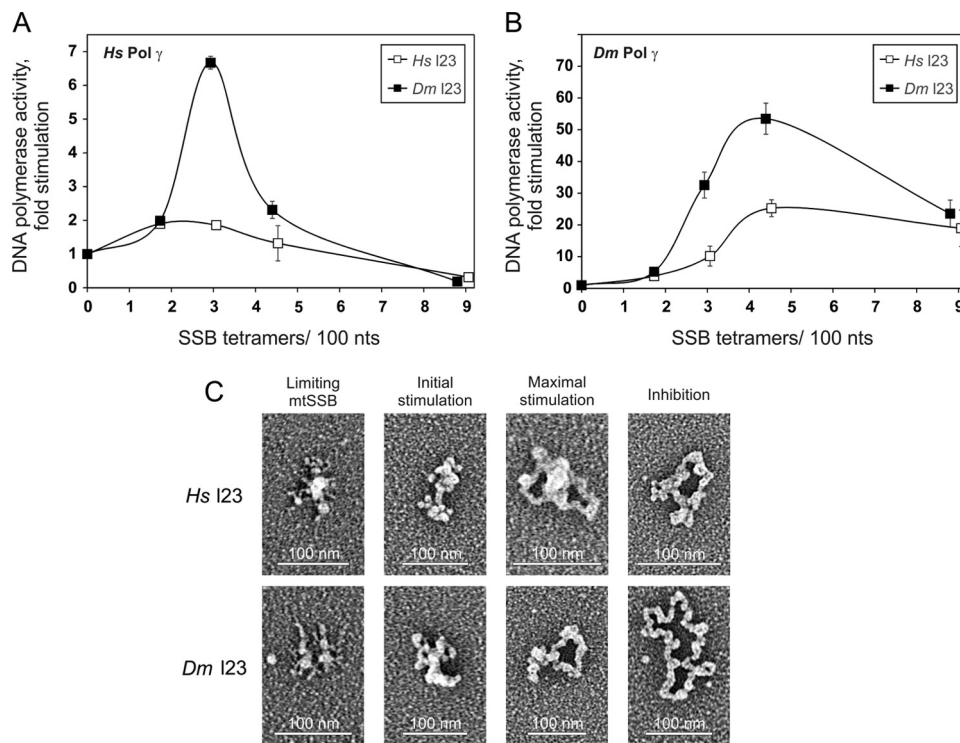


**FIGURE 4. Stimulation of the DNA polymerase activity of Pol  $\gamma$  and template DNA organization by loop 2,3 variants of HsmtSSB and DmmtSSB.** A and B, a DNA polymerase assay was performed as described under "Experimental Procedures," under conditions as described in the legend to Fig. 3A, except that the loop 2,3 mtSSB variants (*H. sapiens* (open squares) or *D. melanogaster* (closed squares)) were used. C, electron microscopy of *H. sapiens* (top) and *D. melanogaster* (bottom) loop 2,3 variants of mtSSB on M13 DNA. The binding reaction was performed at 30 mM KCl and 4 mM MgCl<sub>2</sub>. The images are representative of template species formed at the following ratios of SSB tetramers/100 nucleotides, which correspond to the indicated individual phases of the stimulation of HsPol  $\gamma$  activity: limiting mtSSB, 1.7 Hsl2,3 mtSSB and 1.2 Dml2,3 mtSSB; initial stimulation, 3.4 Hsl2,3 mtSSB and 1.8 Dml2,3 mtSSB; maximal stimulation, 4 Hsl2,3 mtSSB and 2.5 Dml2,3 mtSSB; inhibition, 6.8 Hsl2,3 mtSSB and 7.2 Dml2,3 mtSSB (also see Table 1). Error bars, S.D.

the double-stranded (replicative) M13 genome, with a contour length of 0.071 nm/nt as compared with 0.34 nm/nt, respectively. Our general observation is that the Hsl2,3 variant is less efficient than the wild-type protein in inducing the transition among template DNA forms (e.g. compare the composition of template DNA species of wild-type versus 12,3 HsmtSSB in the initial stimulation phase in Table 1). However, the composition of the template DNA forms generated by the Hsl2,3 variant at the ratio corresponding to the peak of HsPol  $\gamma$  stimulation by the wild-type protein is very similar to that of the wild-type HsmtSSB (compare the respective compositions of template DNA species in Table 1). This implies that the variations observed in the template DNA organization for the Hsl2,3 variant cannot explain fully the loss of its ability to stimulate Pol  $\gamma$ .

DmPol  $\gamma$  is most active when the majority of template DNA molecules are fully open. Thus, the inefficient opening of template DNA species by the Hsl2,3 variant readily explains its inefficiency in stimulating DmPol  $\gamma$ . However, HsPol  $\gamma$  is more active on more dense template DNA species, preferably a mixture of the collapsed and partially open species that Hsl2,3 is able to develop as efficiently as the wild-type protein (see Table 1). Therefore, the inability of Hsl2,3 to stimulate HsPol  $\gamma$  cannot be explained simply by a lack of a specific template DNA species.

Because DmmtSSB is able to stimulate both Pols efficiently, it is possible that its residual loop 2,3 structure is functional. To test this possibility, we generated a loop 2,3 deletion variant of DmmtSSB (Dml2,3) and tested its ability to stimulate the activ-

ity of both Pols (Fig. 4, A and B). We found that the Dml2,3 variant stimulates the activity of both Pols to an extent comparable with the wild-type protein. The stimulation profiles of HsPol  $\gamma$  and DmPol  $\gamma$  obtained with the Dml2,3 variant are similar to those obtained with the wild-type protein (compare Fig. 4 (A and B) with Fig. 3 (A and B)). The only difference we noticed is that the decrease in HsPol  $\gamma$  activity within the inhibition phase of stimulation by Dml2,3 appears to be more dramatic than in the case of the wild-type protein. Specifically, at a ratio of 4–5 SSB tetramers/100 nt in the presence of wild-type DmmtSSB, the -fold stimulation decreases to  $\sim$ 4.5, whereas in the presence of the Dml2,3 variant it drops to  $\sim$ 2.5 (compare Figs. 4A and 3A). Next, we tested whether deletion of the loop 2,3 structure affects the ability of DmmtSSB to organize the template (Fig. 4C). At a ratio of SSB tetramers/100 nt that corresponds to the limiting mtSSB phase of the HsPol  $\gamma$  stimulation profile, the 12,3 variant of DmmtSSB shows no significant changes in the organization of the template DNA molecules. At a ratio corresponding to the initial stimulation phase, we observed an approximately equal contribution of forms leading to the partially open form, which differs from the profile of *D. melanogaster* wild-type protein. At the peak of stimulation, the DmmtSSB 12,3 variant organizes the template DNA into predominantly partially open forms (60%). Notably, the contribution of collapsed forms at this point is relatively low, 16% as compared with 35% for the *D. melanogaster* wild-type protein, whereas the fraction of fully open forms is more substantial at 24% as compared with 12%, respectively. Further increase in the

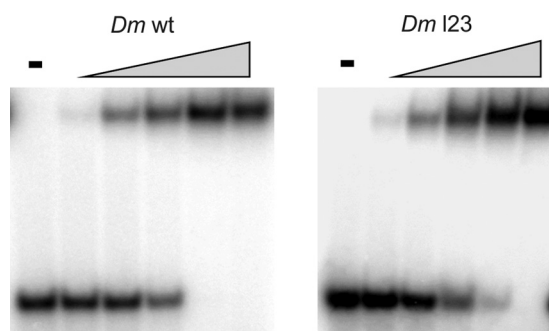


FIGURE 5. **ssDNA binding affinity of DmmtSSB and the loop 2,3 variant.** ssDNA binding affinity was evaluated by a gel mobility shift assay. mtSSBs were preincubated with a radiolabeled 40-mer oligonucleotide at 30 mM KCl in the presence of increasing mtSSB concentrations: 0, 0.5, 1, 2, 4, and 8 nM (as tetramer), as described under "Experimental Procedures." —, no added protein. The fraction of unbound and bound oligomer was quantitated as described under "Experimental Procedures," and the data from two independent experiments were used to determine the apparent  $K_d$  values.

DmmtSSB l2,3 variant concentration increases the fraction of fully open molecules, similar to the wild-type DmmtSSB. Thus, the shift in the fraction of forms toward the fully open species at the peak of stimulation in comparison with those observed for wild-type DmmtSSB may underlie the increased inhibition of HsPol  $\gamma$  activity in the inhibitory phase of stimulation by the Dml2,3 variant.

**mtSSBs Bind ssDNA with Similar Affinity**—To evaluate possible differences in ssDNA binding between the HsmtSSB and DmmtSSB, we examined the ssDNA affinity of the DmmtSSB variants using a gel mobility shift assay (Fig. 5). We estimate the dissociation constant to be  $1.7 \pm 0.06$  nM for *D. melanogaster* WT mtSSB and  $2.54 \pm 0.06$  nM for the Dml2,3 variant. We also re-evaluated the ssDNA binding affinity of the HsmtSSBs and found their apparent  $K_d$  values to be consistent with those we published previously ( $2.26 \pm 0.07$  nM for human WT mtSSB and  $2.2 \pm 0.06$  nM for the Hsl2,3 variant (7)). Overall, we found no significant differences in the ssDNA binding affinity among the mtSSBs.

**Stimulation of Pol  $\gamma$  Activity by *E. coli* SSB Also Depends on Organization of the Template DNA**—EcSSB contains several structural differences as compared with the HsmtSSB and DmmtSSB. It lacks the loop 2,3 structure and contains an  $\sim 60$ -amino acid C-terminal extension that is implicated in interactions with its protein partners. Despite these differences, EcSSB is capable of stimulating both HsPol  $\gamma$  and DmPol  $\gamma$  (7, 22). On the other hand, HsmtSSB is not able to substitute for EcSSB *in vivo* (even in the presence of the C terminus of EcSSB) (28). To evaluate whether this functional divergence could result from a differing ability in template DNA organization, we first examined the EcSSB stimulation profiles of Pol  $\gamma$  and indeed found them to differ from those of the HsmtSSB and DmmtSSB. EcSSB stimulates HsPol  $\gamma$  activity  $\sim 3$ -fold and DmPol  $\gamma$  activity  $\sim 2$ -fold more efficiently than the mtSSBs (Fig. 6, A and B), which is consistent with that observed in previous studies (22, 27). The EcSSB stimulation initiates immediately, and its maximal stimulation is reached at concentrations even lower than those of DmmtSSB. Further increase in the EcSSB concentration does not induce an inhibition phase but maintains the activity of both Pols at their highest efficiency level (plateau

phase). Next we examined how the template DNA is organized at individual phases of the EcSSB stimulation profile (Fig. 6C). At a ratio of 0.85 SSB tetramers/100 nt, almost all template DNA molecules are already either partly collapsed (62%) or collapsed (34%). Such a distribution of these species characterizes the initial stimulation phase of the stimulation profiles of the mtSSBs and correlates well with the immediate increase in the Pol activity. At concentrations between 1.3 and 2.6 EcSSB tetramers/100 nt, the majority of species shift from the collapsed (61%) to the fully open forms (66%). At the ratio of 1.3 SSB tetramers/100 nt, HsPol  $\gamma$  is close to its maximal activity. By comparison, DmPol  $\gamma$  reaches  $\sim 50\%$  of its maximal activity at the EcSSB ratio of 1.3 and reaches its maximum at 2.6. Because the transitions from the collapsed to the fully open forms occur over a relatively short range of EcSSB concentrations, it is difficult to describe accurately the composition of the template DNA species at the maximal stimulation phases for each Pol. However, given the differences observed between the HsPol  $\gamma$  and DmPol  $\gamma$  stimulation profiles, we predict that in the maximal stimulation phase, EcSSB organizes the template DNA in a similar way as do HsmtSSB and DmmtSSB. Nonetheless, in the case of the HsmtSSB and DmmtSSB, the increase in the fully open species correlates with a decrease in the HsPol  $\gamma$  activity (the inhibition phase), whereas this does not appear to be the case for EcSSB. Given that the activity of both Pols is reaching a plateau phase, we conclude that the fully open species generated by EcSSB are utilized efficiently.

We also examined the ssDNA binding affinity of EcSSB under our experimental conditions and obtained a  $K_d$  value of  $2.2$  nM  $\pm 0.05$ , which is similar to that of the mtSSBs. Thus, another property of EcSSB must underlie the differences we observed in its ability to stimulate Pol  $\gamma$ .

## Discussion

In this study, we sought to address whether the stimulation of Pol  $\gamma$  activity by mtSSB occurs due to a direct Pol  $\gamma$ -mtSSB interaction, or indirectly through interaction of mtSSB with the template DNA. Both possibilities find substantial support in published studies on various replication machineries. The replication machinery of bacteriophage T7 shares significant similarities with that of mtDNA (29–32), and a direct interaction of the T7 phage SSB homologue (gp2.5) with the DNA polymerase (gp5) increases the processivity of the replication machinery during leading DNA strand synthesis (33). *E. coli* SSB functions as a loader for DNA Pol III and thus facilitates the bacterial replication process (34). In both cases, the interaction of SSB protein with its cognate Pol is facilitated by an acidic C terminus that is absent in mtSSBs. On the other hand, indirect stimulation of DNA synthesis through binding of the template DNA is well documented for many SSBs, as for phage phi29 gp5, phage T4 gp32, as well as for *E. coli* SSB in stimulating the phi29 DNA pol (35) or for the human nuclear SSB (RPA), T4 gp32, and *E. coli* SSB in stimulating the nuclear replicative DNA pol  $\delta$  (15).

Two mechanisms have been proposed to explain the functional relationship of mitochondrial DNA polymerases with their partner mtSSBs. Previously, we have reported that DmmtSSB enhances primer recognition and binding to primer-

## Mechanism of Stimulation of Pol $\gamma$ Activity by mtSSB

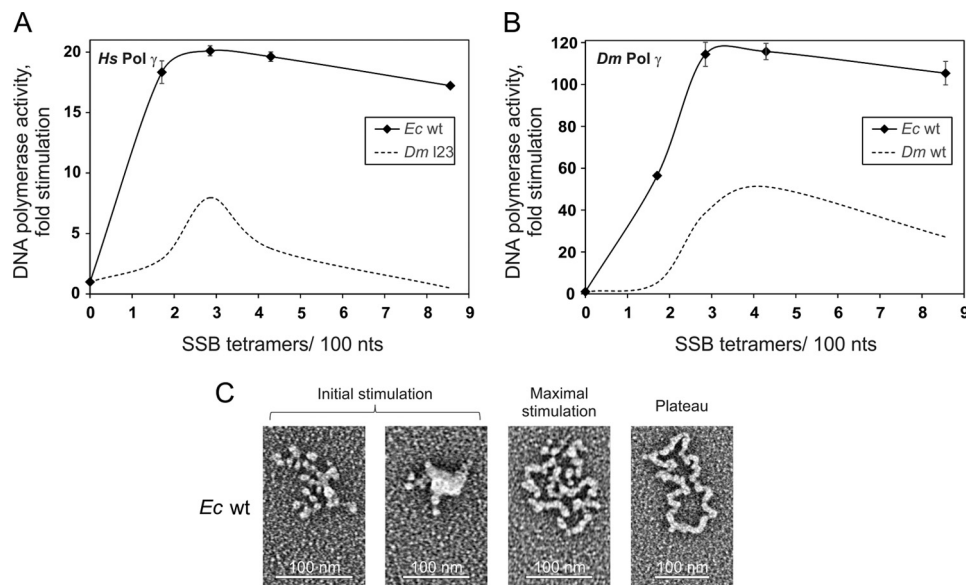


**FIGURE 6. Stimulation of the DNA polymerase activity of Pol  $\gamma$  and template DNA organization by *E. coli* SSB.** A and B, a DNA polymerase assay was performed as described under "Experimental Procedures," as in Fig. 3A except that *Ec*SSB was used (diamonds). Dashed curves, *Dm*mtSSB control. C, electron microscopy of *E. coli* SSB protein on M13 DNA. The binding reaction was performed at 30 mM KCl and 4 mM MgCl<sub>2</sub>. The images are representative of template species formed at the following ratios of SSB tetramers/100 nucleotides, which correspond to the indicated individual phases of the stimulation of *Hs*Pol  $\gamma$  activity: initial stimulation, 0.85 and 1.3; maximal stimulation, 2.6; plateau, 5.1 (also see Table 1). Error bars, S.D.

template DNA and stimulates the rate of initiation of the DNA synthesis of its partner *Dm*Pol  $\gamma$  (12). On the other hand, Mikhailov and Bogenhagen (13) proposed that in the case of the vertebrate system, mtSSB stimulates DNA synthesis by Pol  $\gamma$  mainly by enhancing processivity. The observation we report here that the cross-species stimulation of Pol  $\gamma$  activity is comparably efficient suggests that both systems share similar mechanistic features. We observed that individual phases of stimulation of Pol  $\gamma$  activity occur at specific molar ratios of SSB to template DNA. This finding gives a novel perspective to understanding the interplay of the mtDNA replication components. In our earlier studies investigating the insect system, we employed molar ratios that correspond approximately to the maximal stimulation phase of Pol  $\gamma$  (12) (compare with Fig. 3B), whereas in the studies on the vertebrate system, the highest ratio used corresponds approximately to the limiting phase of the *Hs*mtSSB stimulation profile (13) (compare with Fig. 3A). In light of the results presented here, we conclude that both earlier reports most likely describe the same mechanism as applied to different stages of stimulation of Pol  $\gamma$  activity. The studies presented here appear to exclude the possibility that the mechanism of Pol  $\gamma$  stimulation is based on its direct interaction with its cognate mtSSB, at least on the ssDNA substrate used here, which may not mimic fully lagging strand DNA synthesis as it would occur *in vivo* because there the ssDNA template may be present more transiently. We suggest instead that the enhanced primer recognition described for the insect system is probably a consequence of passive organization of the ssDNA with increasing mtSSB concentration. At the same time, this effect explains the apparent lack of enhanced primer recognition in the study on the vertebrate system because it emerges at higher ratios of SSB to template DNA.

Our electron microscopic analysis demonstrates that the efficiency of template DNA organization by SSB varies between

species; in other words, *Hs*mtSSB requires >6 tetramers/100 nt to open fully ~50% of the template DNA molecules, whereas *Dm*mtSSB and *Ec*SSB require ~3.5 and ~2.5 tetramers/100 nt to open ~80 and ~65% of the template DNA molecules, respectively, and this difference appears to mirror the differences in the Pol  $\gamma$  stimulation efficiency by these SSBs. Despite these differences, for each of the SSBs analyzed, the comparative stimulation phases correspond visually with the same composition of template DNA species. This provides a clear correlation between Pol  $\gamma$  activity and template DNA organization. We propose that organization of the template DNA is the major factor contributing to the stimulation of Pol  $\gamma$  activity in both insect and human mtDNA replication. Furthermore, it seems likely that a relationship between template organization and stimulation of DNA synthesis may extend to other systems, including chromosomal replication in both prokarya and eukarya. Historically, however, EM images of various SSBs and, in particular, the *E. coli* SSB or the *S. cerevisiae* replication protein A heterotrimer bound to ssDNA, have emphasized the fully extended forms, probably because they are visually striking and more "regular" in appearance than the partially opened forms that occur at lower ratios of protein to DNA (36), (37). Our study provides a clear demonstration that these fully extended forms with a smooth, regular protein coating along the ssDNA are in fact suboptimal substrates with regard to stimulation of Pol  $\gamma$  activity.

In evaluating how the interaction of mtSSB with template DNA relates to Pol  $\gamma$  activity, we found that the human enzyme utilizes preferentially compacted templates (a mixture of collapsed and partially open species), whereas the insect enzyme achieves its maximal activity on open templates (a mixture of partially and fully open species). This finding emphasizes the importance of template DNA organization in modulating Pol  $\gamma$  activity. The different preferences for the template DNA orga-



nization of the *D. melanogaster* and *H. sapiens* polymerases underscore differences in their biochemical properties. We demonstrated *DmPol*  $\gamma$  to have significantly lower activity than *HsPol*  $\gamma$  in the absence of SSB. Stimulation by SSB compensates for this difference, and at the phase of maximal stimulation, both Pols produce a comparable amount of the nascent DNA. Also, despite the differences between the cross-species stimulation profiles, the species-specific profiles show that comparable SSB concentrations are required for the corresponding phases of stimulation to occur. This suggests that the requisite properties of the cognate mtSSBs and Pols  $\gamma$  adapted mutually in the evolution process. The lower activity of *DmPol*  $\gamma$  in the absence of SSB may result from its lower affinity for the template DNA and/or weaker ability to disrupt secondary structural elements within ssDNA template. Indeed, we reported recently a comparative analysis of Pol  $\gamma$  sequences from various metazoan taxa that revealed several structural differences between the enzymes of vertebrata and other metazoan taxa, some of which may explain differences in interactions with the template DNA (17). In particular, residues His<sup>320</sup>, Lys<sup>327</sup>, Lys<sup>331</sup>, and Lys<sup>335</sup> of the newly identified exonuclease motif (Lys<sup>319</sup>–Ser<sup>344</sup>) in the catalytic subunit of human Pol  $\gamma$  (Pol  $\gamma\alpha$ ), absent in protostome homologs, locate in close proximity to the minor groove of the primer-template DNA modeled at the Pol  $\gamma\alpha$  binding site (38). The precise role of these residues remains to be investigated, but given their location and positive charge, we predict that they enhance the DNA binding affinity of the enzyme. Furthermore, it has been demonstrated that the dimeric accessory subunit of *HsPol*  $\gamma$  (Pol  $\gamma\beta$ ) enhances the ssDNA binding affinity of Pol  $\gamma\alpha$  by  $\sim$ 100-fold and increases its processivity by 50–100-fold (31, 39). Given that the insect Pol  $\gamma$  contains a monomeric Pol  $\gamma\beta$ , the differences we observe in their interactions with the template DNA may also reflect differences in the contributions of Pol  $\gamma\beta$  to the properties of the holoenzyme (17). In that regard, it has been demonstrated that mutations within the dimerization interface of human Pol  $\gamma\beta$ , which is absent in the insect homologue, result in decreased formation of a productive Pol  $\gamma$ -DNA complex, resulting in a lower processivity of the enzyme (17, 40). Different properties of the *D. melanogaster* and *H. sapiens* polymerases  $\gamma$  might also be extrapolated to the mtDNA replication process to suggest that although the overall efficiency of DNA synthesis in both systems is probably similar, the mechanism of initiation of DNA strand synthesis may differ.

We demonstrated previously that the loop 2,3 structure of *HsmtSSB* is important for the stimulation of *HsPol*  $\gamma$  activity and proposed a putative direct interaction of this element with the *HsPol*  $\gamma$  (7). Here, we found that *DmmtSSB* as well as its I2,3 variant efficiently stimulate *HsPol*  $\gamma$ , arguing that the role served by the loop 2,3 structure in the stimulation mechanism most likely does not require its direct interaction with Pol  $\gamma$ . Rather, the I2,3 variant of *HsmtSSB* fails to stimulate efficiently either *HsPol*  $\gamma$  or *DmPol*  $\gamma$ , suggesting that its role is more general. Our previous studies showed that deletion of loop 2,3 does not alter ssDNA binding affinity. Indeed, we show here that *Hsl2,3* is able to bind template DNA molecules to form collapsed and partially open template species, but in contrast to the wild-type protein, it is incapable of opening the template

DNA molecules fully (at least over the concentration range evaluated). We have examined the ssDNA binding affinities of all of the SSB variants and found no significant differences between them. This argues that the loop 2,3 structure facilitates a property of *HsmtSSB* other than ssDNA binding that is involved in modulation of template DNA organization and indirectly in the stimulation of Pol  $\gamma$ . This in turn suggests that the protein-DNA complexes formed by the *Hsl2,3* variant that fails to stimulate *HsPol*  $\gamma$  have altered molecular properties, which could explain why the *Hsl2,3* variant generates mixtures of collapsed and partially open species that are visually similar to those that correspond to the maximal stimulation phase of *HsPol*  $\gamma$  by wild-type *HsmtSSB*.

Our electron microscopic observations argue that under the experimental conditions used, the SSB proteins saturate the template DNA at an approximate ratio of 3 tetramers/100 nt (by calculation), which corresponds to the 35-nt binding mode described previously for *EcSSB* (41). However, as demonstrated previously for *EcSSB*, the binding mode may transit through several intermediate modes to a 65-nt binding mode. Such a transition is related generally with increased salt concentration but also occurs at low SSB concentrations (41). Although our analysis does not allow evaluation of these transitions directly, we observe that the stimulation of *HsPol*  $\gamma$  activity corresponds with a transition from the collapsed to a less dense species. Interestingly, recent studies on replication restart in bacteria have shown that the 65-nt binding mode can be reverted actively to the 35-nt binding mode by interaction with the protein machinery required for reinitiating prematurely terminated replication (42). Despite its similar DNA binding affinity and mode of DNA binding, *HsmtSSB* stimulates Pol  $\gamma$  activity and facilitates template DNA opening at concentrations exceeding that required for template saturation, whereas for *DmSSB* and *EcSSB*, template saturation corresponds roughly to the maximal stimulation phase and the transition from partially to fully open template molecules. This difference might suggest that protein-protein interaction between neighboring tetramers could contribute to the organization of the template DNA by *HsmtSSB*. Notably, the 35-nt binding mode of *EcSSB* imparts high cooperativity, whereas cooperativity in the 65-nt binding mode is limited (41). Earlier data suggest that *HsmtSSB* is less cooperative than *EcSSB* (43). Interestingly, *EcSSB* and *DmmtSSB* lack the loop 2,3 structure, which appears dispensable for efficient template DNA organization and stimulation of Pol  $\gamma$  by these proteins, whereas its presence is critical for *HsmtSSB* function. Thus, a role for the loop 2,3 structure in interaction between neighboring tetramers and cooperative ssDNA binding could explain why the *Hsl2,3* variant is incapable of developing the fully open template species.

We show that template DNA molecules opened fully by *DmmtSSB* are inhibitory for *DmPol*  $\gamma$ , whereas visually, the same species generated by the *HsSSB* and *EcSSB* are not. This again suggests that despite their visual resemblance, the DNA-protein complexes formed by the three SSBs may have different molecular properties. Pol  $\gamma$  must displace bound SSB molecules as it copies the template DNA strand, so it is also feasible that the three SSBs are displaced by the *H. sapiens* and *D. melanogaster* polymerases with different efficiencies. This may require

## Mechanism of Stimulation of Pol $\gamma$ Activity by mtSSB

a transient physical Pol  $\gamma$ -SSB interaction, and at present, our results do not address this possibility.

In summary, our data support a general mechanism for the stimulation of Pol  $\gamma$  activity by mtSSB. We have shown for the first time a relationship between Pol  $\gamma$  activity and the SSB-generated template DNA organization that provides novel insight into understanding a mechanism of indirect stimulation. Although we propose the general mechanism by which this occurs, several differences between insect and vertebrate systems have emerged. Together with our comparative analysis of Pol  $\gamma$  sequences and structural organization from various metazoan taxa (17), we provide evidence of both commonality and distinctions as they may relate to lagging strand DNA synthesis *per se*, emphasizing the strength of combined biochemical and evolutionary approaches in studies of animal mtDNA replication.

**Author Contributions**—G. L. C. and L. S. K. designed the biochemical experiments and wrote the paper. G. L. C., F. A. R., S. L. H., and O. J. N. performed the biochemical experiments. O. B. and J. D. G. designed and performed the electron microscopic experiments and edited the manuscript. G. L. C., L. S. K., O. B., and J. G. analyzed the results, and all authors approved the final version of the manuscript.

**Acknowledgment**—We thank Aysegül Dede for help in the EM analysis.

### References

1. Rajala, N., Gerhold, J. M., Martinsson, P., Klymov, A., and Spelbrink, J. N. (2014) Replication factors transiently associate with mtDNA at the mitochondrial inner membrane to facilitate replication. *Nucleic Acids Res.* **42**, 952–967
2. Korhonen, J. A., Pham, X. H., Pellegrini, M., and Falkenberg, M. (2004) Reconstitution of a minimal mtDNA replisome *in vitro*. *EMBO J.* **23**, 2423–2429
3. Ruhanen, H., Borrie, S., Szabadkai, G., Tyynismaa, H., Jones, A. W., Kang, D., Taanman, J. W., and Yasukawa, T. (2010) Mitochondrial single-stranded DNA binding protein is required for maintenance of mitochondrial DNA and 7S DNA but is not required for mitochondrial nucleoid organisation. *Biochim. Biophys. Acta* **1803**, 931–939
4. Farr, C. L., Matsushima, Y., Lagina, A. T., 3rd, Luo, N., and Kaguni, L. S. (2004) Physiological and biochemical defects in functional interactions of mitochondrial DNA polymerase and DNA-binding mutants of single-stranded DNA-binding protein. *J. Biol. Chem.* **279**, 17047–17053
5. Maier, D., Farr, C. L., Poeck, B., Alahari, A., Vogel, M., Fischer, S., Kaguni, L. S., and Schneuwly, S. (2001) Mitochondrial single-stranded DNA-binding protein is required for mitochondrial DNA replication and development in *Drosophila melanogaster*. *Mol. Biol. Cell* **12**, 821–830
6. Takamatsu, C., Umeda, S., Ohsato, T., Ohno, T., Abe, Y., Fukuoh, A., Shinagawa, H., Hamasaki, N., and Kang, D. (2002) Regulation of mitochondrial D-loops by transcription factor A and single-stranded DNA-binding protein. *EMBO Rep.* **3**, 451–456
7. Oliveira, M. T., and Kaguni, L. S. (2011) Reduced stimulation of recombinant DNA polymerase  $\gamma$  and mitochondrial DNA (mtDNA) helicase by variants of mitochondrial single-stranded DNA-binding protein (mtSSB) correlates with defects in mtDNA replication in animal cells. *J. Biol. Chem.* **286**, 40649–40658
8. Jemt, E., Farge, G., Bäckström, S., Holmlund, T., Gustafsson, C. M., and Falkenberg, M. (2011) The mitochondrial DNA helicase TWINKLE can assemble on a closed circular template and support initiation of DNA synthesis. *Nucleic Acids Res.* **39**, 9238–9249
9. Zhou, R., Kozlov, A. G., Roy, R., Zhang, J., Korolev, S., Lohman, T. M., and Ha, T. (2011) SSB functions as a sliding platform that migrates on DNA via reptation. *Cell* **146**, 222–232
10. Kozlov, A. G., Jezewska, M. J., Bujalowski, W., and Lohman, T. M. (2010) Binding specificity of *Escherichia coli* single-stranded DNA binding protein for the  $\chi$  subunit of DNA pol III holoenzyme and PriA helicase. *Biochemistry* **49**, 3555–3566
11. Meyer, R. R., and Laine, P. S. (1990) The single-stranded DNA-binding protein of *Escherichia coli*. *Microbiol. Rev.* **54**, 342–380
12. Farr, C. L., Wang, Y., and Kaguni, L. S. (1999) Functional interactions of mitochondrial DNA polymerase and single-stranded DNA-binding protein: template-primer DNA binding and initiation and elongation of DNA strand synthesis. *J. Biol. Chem.* **274**, 14779–14785
13. Mikhailov, V. S., and Bogenhagen, D. F. (1996) Effects of *Xenopus laevis* mitochondrial single-stranded DNA-binding protein on primer-template binding and 3'  $\rightarrow$  5' exonuclease activity of DNA polymerase  $\gamma$ . *J. Biol. Chem.* **271**, 18939–18946
14. Korhonen, J. A., Gaspari, M., and Falkenberg, M. (2003) TWINKLE has 5'  $\rightarrow$  3' DNA helicase activity and is specifically stimulated by mitochondrial single-stranded DNA-binding protein. *J. Biol. Chem.* **278**, 48627–48632
15. Kenny, M. K., Lee, S. H., and Hurwitz, J. (1989) Multiple functions of human single-stranded-DNA binding protein in simian virus 40 DNA replication: single-strand stabilization and stimulation of DNA polymerases  $\alpha$  and  $\delta$ . *Proc. Natl. Acad. Sci. U.S.A.* **86**, 9757–9761
16. Copeland, W. C. (2014) Defects of mitochondrial DNA replication. *J. Child Neurol.* **29**, 1216–1224
17. Oliveira, M. T., Haukka, J., and Kaguni, L. S. (2015) Evolution of the metazoan mitochondrial replicase. *Genome Biol. Evol.* **7**, 943–959
18. Williams, A. J., Wernet, C. M., and Kaguni, L. S. (1993) Processivity of mitochondrial DNA polymerase from *Drosophila* embryos: effects of reaction conditions and enzyme purity. *J. Biol. Chem.* **268**, 24855–24862
19. Oliveira, M. T., and Kaguni, L. S. (2010) Functional roles of the N- and C-terminal regions of the human mitochondrial single-stranded DNA-binding protein. *PLoS One* **5**, e15379
20. Oliveira, M. T., and Kaguni, L. S. (2009) Comparative purification strategies for *Drosophila* and human mitochondrial DNA replication proteins: DNA polymerase  $\gamma$  and mitochondrial single-stranded DNA-binding protein. *Methods Mol. Biol.* **554**, 37–58
21. Griffith, J. D., and Christiansen, G. (1978) Electron microscope visualization of chromatin and other DNA-protein complexes. *Annu. Rev. Biophys. Bioeng.* **7**, 19–35
22. Williams, A. J., and Kaguni, L. S. (1995) Stimulation of *Drosophila* mitochondrial DNA polymerase by single-stranded DNA-binding protein. *J. Biol. Chem.* **270**, 860–865
23. Johnson, A. A., and Johnson, K. A. (2001) Fidelity of nucleotide incorporation by human mitochondrial DNA polymerase. *J. Biol. Chem.* **276**, 38090–38096
24. Wong, T. S., Rajagopalan, S., Townsley, F. M., Freund, S. M., Petrovich, M., Loakes, D., and Fersht, A. R. (2009) Physical and functional interactions between human mitochondrial single-stranded DNA-binding protein and tumour suppressor p53. *Nucleic Acids Res.* **37**, 568–581
25. Hoke, G. D., Pavco, P. A., Ledwith, B. J., and Van Tuyle, G. C. (1990) Structural and functional studies of the rat mitochondrial single strand DNA binding protein P16. *Arch. Biochem. Biophys.* **282**, 116–124
26. Yang, C., Curth, U., Urbanke, C., and Kang, C. (1997) Crystal structure of human mitochondrial single-stranded DNA binding protein at 2.4 Å resolution. *Nat. Struct. Biol.* **4**, 153–157
27. Thömmes, P., Farr, C. L., Marton, R. F., Kaguni, L. S., and Cotterill, S. (1995) Mitochondrial single-stranded DNA-binding protein from *Drosophila* embryos: physical and biochemical characterization. *J. Biol. Chem.* **270**, 21137–21143
28. Curth, U., Genschel, J., Urbanke, C., and Greipel, J. (1996) *In vitro* and *in vivo* function of the C-terminus of *Escherichia coli* single-stranded DNA binding protein. *Nucleic Acids Res.* **24**, 2706–2711
29. Copeland, W. C., Pomarev, M. V., Nguyen, D., Kunkel, T. A., and Longley, M. J. (2003) Mutations in DNA polymerase  $\gamma$  cause error prone DNA synthesis in human mitochondrial disorders. *Acta Biochim. Pol.* **50**, 155–167
30. Luo, N., and Kaguni, L. S. (2005) Mutations in the spacer region of *Drosophila* mitochondrial DNA polymerase affect DNA binding, processivity,

- and the balance between Pol and Exo function. *J. Biol. Chem.* **280**, 2491–2497
31. Fan, L., Kim, S., Farr, C. L., Schaefer, K. T., Randolph, K. M., Tainer, J. A., and Kaguni, L. S. (2006) A novel processive mechanism for DNA synthesis revealed by structure, modeling and mutagenesis of the accessory subunit of human mitochondrial DNA polymerase. *J. Mol. Biol.* **358**, 1229–1243
  32. Spelbrink, J. N., Li, F. Y., Tiranti, V., Nikali, K., Yuan, Q. P., Tariq, M., Wanrooij, S., Garrido, N., Comi, G., Morandi, L., Santoro, L., Toscano, A., Fabrizi, G. M., Somer, H., Croxen, R., Beeson, D., Poulton, J., Suomalainen, A., Jacobs, H. T., Zeviani, M., and Larsson, C. (2001) Human mitochondrial DNA deletions associated with mutations in the gene encoding Twinkle, a phage T7 gene 4-like protein localized in mitochondria. *Nat. Genet.* **28**, 223–231
  33. Ghosh, S., Hamdan, S. M., and Richardson, C. C. (2010) Two modes of interaction of the single-stranded DNA-binding protein of bacteriophage T7 with the DNA polymerase-thioredoxin complex. *J. Biol. Chem.* **285**, 18103–18112
  34. Glover, B. P., and McHenry, C. S. (1998) The  $\chi$   $\psi$  subunits of DNA polymerase III holoenzyme bind to single-stranded DNA-binding protein (SSB) and facilitate replication of an SSB-coated template. *J. Biol. Chem.* **273**, 23476–23484
  35. Gutiérrez, C., Martín, G., Sogo, J. M., and Salas, M. (1991) Mechanism of stimulation of DNA replication by bacteriophage  $\phi$  29 single-stranded DNA-binding protein p5. *J. Biol. Chem.* **266**, 2104–2111
  36. Alani, E., Thresher, R., Griffith, J. D., and Kolodner, R. D. (1992) Characterization of DNA-binding and strand-exchange stimulation properties of  $\gamma$ -RPA, a yeast single-strand-DNA-binding protein. *J. Mol. Biol.* **227**, 54–71
  37. Chrysogelos, S., and Griffith, J. (1982) *Escherichia coli* single-strand binding protein organizes single-stranded DNA in nucleosome-like units. *Proc. Natl. Acad. Sci. U.S.A.* **79**, 5803–5807
  38. Euro, L., Farnum, G. A., Palin, E., Suomalainen, A., and Kaguni, L. S. (2011) Clustering of Alpers disease mutations and catalytic defects in biochemical variants reveal new features of molecular mechanism of the human mitochondrial replicase, Pol  $\gamma$ . *Nucleic Acids Res.* **39**, 9072–9084
  39. Yakubovskaya, E., Chen, Z., Carrodegua, J. A., Kisker, C., and Bogenhagen, D. F. (2006) Functional human mitochondrial DNA polymerase  $\gamma$  forms a heterotrimer. *J. Biol. Chem.* **281**, 374–382
  40. Lee, Y. S., Lee, S., Demeler, B., Molineux, I. J., Johnson, K. A., and Yin, Y. W. (2010) Each monomer of the dimeric accessory protein for human mitochondrial DNA polymerase has a distinct role in conferring processivity. *J. Biol. Chem.* **285**, 1490–1499
  41. Lohman, T. M., and Ferrari, M. E. (1994) *Escherichia coli* single-stranded DNA-binding protein: multiple DNA-binding modes and cooperativities. *Annu. Rev. Biochem.* **63**, 527–570
  42. Bhattacharyya, B., George, N. P., Thurmes, T. M., Zhou, R., Jani, N., Wesel, S. R., Sandler, S. J., Ha, T., and Keck, J. L. (2014) Structural mechanisms of PriA-mediated DNA replication restart. *Proc. Natl. Acad. Sci. U.S.A.* **111**, 1373–1378
  43. Curth, U., Urbanke, C., Greipel, J., Gerberding, H., Tiranti, V., and Zeviani, M. (1994) Single-stranded-DNA-binding proteins from human mitochondria and *Escherichia coli* have analogous physicochemical properties. *Eur. J. Biochem.* **221**, 435–443